

An improvement of direct torque controlled PMSM drive using PWM technique and kalman filter

Dung Quang Nguyen¹, Hau Huu Vo², Pavel Brandstetter³

¹Department of Automation and Control Engineering, Faculty of Electrical and Electronics Engineering, Ton Duc Thang University, Ho Chi Minh City, Vietnam

²Modeling Evolutionary Algorithms Simulation and Artificial Intelligence, Faculty of Electrical and Electronics Engineering, Ton Duc Thang University, Ho Chi Minh City, Vietnam

³Department of Electronics, Faculty of Electrical Engineering and Computer Science, VSB–Technical University of Ostrava, Czech Republic

Article Info

Article history:

Received Sep 3, 2022

Revised Dec 16, 2022

Accepted Feb 3, 2023

Keywords:

Direct torque control

Performance indices

PMSM drive

Pulse width modulation

Kalman filter

ABSTRACT

The paper describes pulse width modulation (PWM) technique and Kalman filter (KF) process to improve performance of direct torque controlled permanent magnet synchronous motor (DTC-PMSM) drive. Performance of DTC methods are strongly affected by high stator current ripple. For lowering the ripple, high switching frequency space vector PWM and KF are utilized in the paper. Mathematical model of PMSM and calculations of important quantities of DTC applied to PMSM drive are presented in the first part. The second part shows computation process of space vector PWM and KF. Performance indices are utilized to evaluate the drive structures. Theoretical assumptions are validated via simulations with Gaussian noised stator current measurement.

This is an open access article under the [CC BY-SA](https://creativecommons.org/licenses/by-sa/4.0/) license.



Corresponding Author:

Hau Huu Vo

Modeling Evolutionary Algorithms Simulation and Artificial Intelligence,

Faculty of Electrical and Electronics Engineering, Ton Duc Thang University

No. 19 Nguyen Huu Tho Street, Tan Phong Ward, District 7, Ho Chi Minh City, Vietnam

Email: vohuuha@tdtu.edu.vn

1. INTRODUCTION

Industrial applications required high mechanical accuracy such as computer-numerical-control machines, robotics, electric vehicles utilizing permanent magnet synchronous motors (PMSMs) because of their high power, low moment of inertia, high start-up torque [1]. Similarly to induction motor drive (IMD), field-oriented-control (FOC) and direct torque control (DTC) strategies [2], [3] are used in high-performance torque and flux controls of PMSM drive [4], [5]. The DTC has a simpler structure than FOC, therefore its simulation and real implementation are easier than FOC. This strategy also gives high robustness and fast response of torque [1], [5].

Conventional DTC methods bring high torque and current ripples because they utilize look-up tables for desired voltages to control the flux and torque [3], [5]. Besides that, they make switching frequency of power converters not constant, even though it was fixed. Integrating pulse-width modulation (PWM) into DTC makes switching frequency constant, and provides improved performance of the torque and the current [6]-[17]. Popular PWM methods are sinusoidal PWM (SPWM) [6]-[8] and space vector PWM (SVPWM) [8]-[10], [12]-[14]. The SVPWM offers a better dc-link utilization of 15% compared to the SPWM [7].

In PMSM drive, measurement stator current errors affect performance of DTC strategies [18]. kalman filter (KF) and its variations have many applications listed in [19]. KF were employed to observe

speed and load [20], estimate currents and their time derivatives [21], [22], identify flux and inductances variation [23], estimate parameter combinations [24]. Forgetting factor was employed to compute noise covariance in dual adaptive KF algorithms [20]. Time derivatives of stator current were provided by KF in model reference adaptive system-based sensorless IMD [21]. Stator currents were estimated by extended KF (EKF) in sensorless PMSM drive [22]. Least squares method was utilized together with EKF to obtain PMSM parameters [23]. Two KF strategies were employed to estimate online any identifiable electrical parameter combinations [24]. Future observations and error minimization of variables were estimated by EKF for controller design [25]. In the paper, estimations and identifications are omitted, instead of that KF is employed to provide approximation of stator currents distorted by Gaussian measurement noises.

2. MATHEMATICAL MODEL OF DTC-PMSM DRIVE

Figure 1 shows control structure of DTC PMSM drive with PWM and KF. In (1)-(4) describe mathematical model of PMSM in $[\alpha, \beta]$ coordinate system:

$$u_{s\alpha} = \frac{d\psi_{s\alpha}}{dt} + i_{s\alpha}R_s \tag{1}$$

$$u_{s\beta} = \frac{d\psi_{s\beta}}{dt} + i_{s\beta}R_s \tag{2}$$

$$\psi_{s\alpha} = L_s i_{s\alpha} + \psi_M \cos \theta_r \tag{3}$$

$$\psi_{s\beta} = L_s i_{s\beta} + \psi_M \sin \theta_r \tag{4}$$

Where $u_{s\alpha}, u_{s\beta}$ are stator voltage vector components; $\psi_{s\alpha}, \psi_{s\beta}$ are stator flux vector components; $i_{s\alpha}, i_{s\beta}$ are stator current vector components; θ_r is rotor position; R_s is stator resistance; L_s is stator inductance; ψ_M is magnetic flux of the PM. In (5) calculates motor torque T_e from stator flux and stator current components, and mechanical relation of motor torque, load torque T_L , and mechanical speed ω_m is expressed by (6):

$$T_e = 1.5p(i_{s\beta}\psi_{s\alpha} - i_{s\alpha}\psi_{s\beta}) \tag{5}$$

$$\frac{d\omega_m}{dt} = \frac{(T_e - T_L)}{J_m} \tag{6}$$

Where p is number of pole pairs, and J_m is motor inertia.

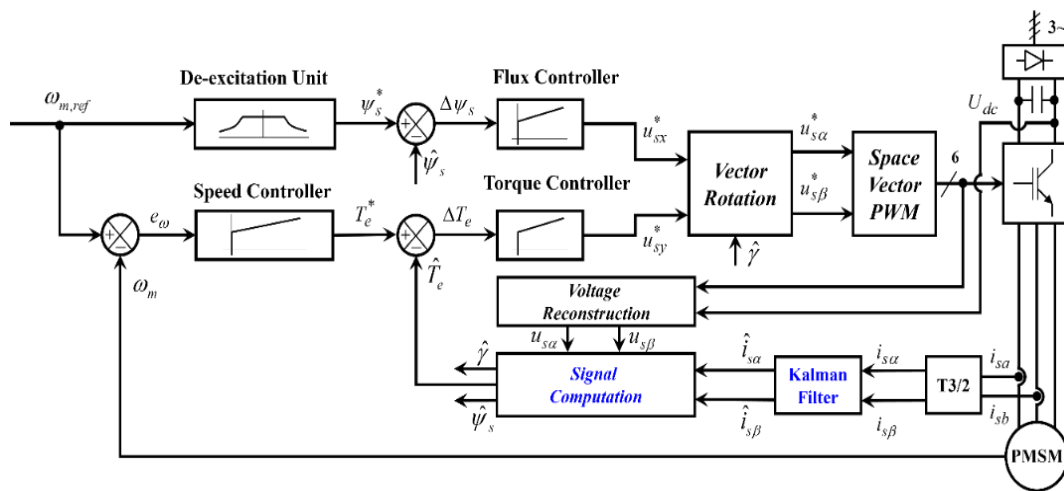


Figure 1. Control structure of DTC PMSM drive with PWM and KF

Signal computation block estimates stator flux components, stator flux vector magnitude, orienting angle γ , motor torque utilizing reconstructed stator voltages and Kalman filtered stator currents, according to (7)-(11):

$$\hat{\psi}_{s\alpha} = \int (u_{s\alpha} - R_s \hat{i}_{s\alpha}) dt \tag{7}$$

$$\hat{\psi}_{s\beta} = \int (u_{s\beta} - R_s \hat{i}_{s\beta}) dt \tag{8}$$

$$\hat{\psi}_s = \sqrt{\hat{\psi}_{s\alpha}^2 + \hat{\psi}_{s\beta}^2} \tag{9}$$

$$\hat{\gamma} = \arcsin\left(\frac{\hat{\psi}_{s\beta}}{\hat{\psi}_s}\right) \tag{10}$$

$$\hat{T}_e = 1.5p(\hat{\psi}_{s\alpha} \hat{i}_{s\beta} - \hat{\psi}_{s\beta} \hat{i}_{s\alpha}) \tag{11}$$

Where symbol ^ denotes estimated quantities. KF block smooths stator current components distorted by Gaussian measurement noises [19]. Next section describes the SVPWM and the KF.

3. COMPUTATION PROCESS OF SPACE VECTOR PWM AND KF

In order to obtain the average value of space vector with desired $u_{s\alpha}$, $u_{s\beta}$ components, PWM techniques are utilized to provide switch-on and switch-off durations of power electronic devices of the inverter. For the SVPWM technique, in one switching period t_s , durations t_a , t_b , t_0 that are respectively time intervals of using vectors U_a , U_b , U_0 (V_0 or V_7) in Figure 2(a), are computed by (12)-(16):

$$\bar{U}^* = \sqrt{(u_{s\alpha}^*)^2 + (u_{s\beta}^*)^2} \tag{12}$$

$$\alpha = \tan^{-1}\left(\frac{u_{s\beta}^*}{u_{s\alpha}^*}\right) \tag{13}$$

$$t_a = t_s \left\{ \cos \alpha \sin\left(\frac{s_k \pi}{3}\right) - \sin \alpha \cos\left(\frac{s_k \pi}{3}\right) \right\} \frac{\sqrt{3} \bar{U}^*}{U_{dc}} \tag{14}$$

$$t_b = t_s \left\{ -\cos \alpha \sin\left[\frac{(s_k - 1)\pi}{3}\right] + \sin \alpha \cos\left[\frac{(s_k - 1)\pi}{3}\right] \right\} \frac{\sqrt{3} \bar{U}^*}{U_{dc}} \tag{15}$$

$$t_0 = t_s - t_a - t_b \tag{16}$$

Where s_k is sector (1 to 6). Figure 2(b) shows that SVPWM utilizes better DC link voltage U_{dc} than SPWM, so the SVPWM is implemented in this paper. Switching combination in Table 1 is employed to reduce loss due to change state of power electronic devices.

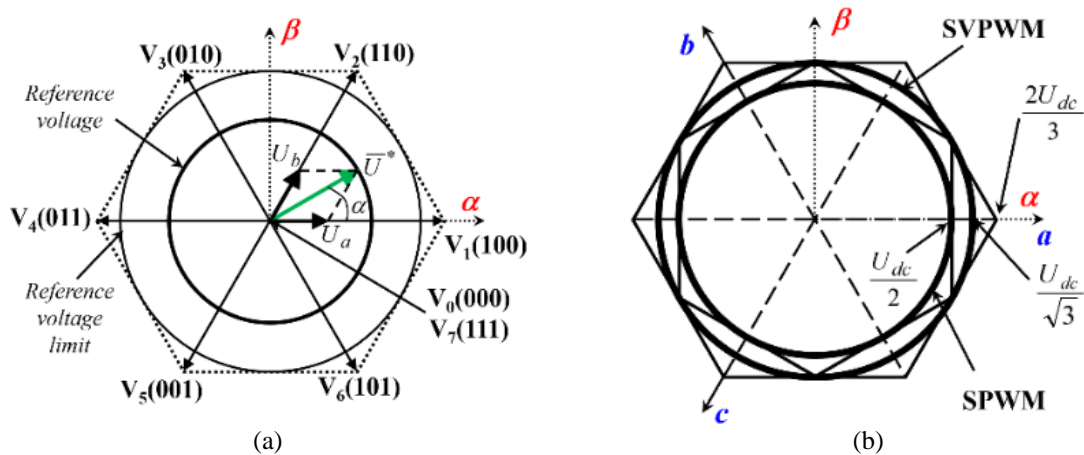


Figure 2. SVPWM method [7] (a) phase vector & reference trajectory and (b) comparison with SPWM method on maximum linear control voltage

Table 1. Switching combination of SVPWM [7]

Sector	1	2	3	4	5	6
Upper switches (S ₁ , S ₃ , S ₅)	S ₁ =t _a +t _b +t ₀ /2 S ₃ =t _b +t ₀ /2 S ₅ =t ₀ /2	S ₁ =t _a +t ₀ /2 S ₃ =t _a +t _b +t ₀ /2 S ₅ =t ₀ /2	S ₁ =t ₀ /2 S ₃ =t _a +t _b +t ₀ /2 S ₅ =t _b +t ₀ /2	S ₁ =t ₀ /2 S ₃ =t _a +t ₀ /2 S ₅ =t _a +t _b +t ₀ /2	S ₁ =t _b +t ₀ /2 S ₃ =t ₀ /2 S ₅ =t _a +t _b +t ₀ /2	S ₁ =t _a +t _b +t ₀ /2 S ₃ =t ₀ /2 S ₅ =t _a +t ₀ /2
Lower switches (S ₄ , S ₆ , S ₂)	S ₄ =t ₀ /2 S ₆ =t _a +t ₀ /2 S ₂ =t _a +t _b +t ₀ /2	S ₄ =t _b +t ₀ /2 S ₆ =t ₀ /2 S ₂ =t _a +t _b +t ₀ /2	S ₄ =t _a +t _b +t ₀ /2 S ₆ =t ₀ /2 S ₂ =t _a +t ₀ /2	S ₄ =t _a +t _b +t ₀ /2 S ₆ =t _b +t ₀ /2 S ₂ =t ₀ /2	S ₄ =t _a +t ₀ /2 S ₆ =t _a +t _b +t ₀ /2 S ₂ =t ₀ /2	S ₄ =t ₀ /2 S ₆ =t _a +t _b +t ₀ /2 S ₂ =t _b +t ₀ /2

The KF block brings estimate of stator current $i_{s\alpha}$, $i_{s\beta}$ components according to (17)-(24):

$$\mathbf{x}_k = \mathbf{F}\mathbf{x}_{k-1} \quad (17)$$

$$\mathbf{y}_k = \mathbf{H}\mathbf{x}_k + \mathbf{v}_k \quad (18)$$

$$\tilde{\mathbf{x}}_k = \mathbf{F}\tilde{\mathbf{x}}_{k-1} \quad (19)$$

$$\tilde{\mathbf{P}}_k = \mathbf{F}\tilde{\mathbf{P}}_{k-1}\mathbf{F}^T \quad (20)$$

$$\tilde{\mathbf{z}}_k = \mathbf{y}_k - \mathbf{H}\tilde{\mathbf{x}}_k \quad (21)$$

$$\mathbf{K}_k = \tilde{\mathbf{P}}_k\mathbf{H}^T(\mathbf{H}\tilde{\mathbf{P}}_k\mathbf{H}^T + \mathbf{R})^{-1} \quad (22)$$

$$\hat{\mathbf{x}}_k = \tilde{\mathbf{x}}_k + \mathbf{K}_k\tilde{\mathbf{z}}_k \quad (23)$$

$$\hat{\mathbf{P}}_k = (\mathbf{I} - \mathbf{K}_k\mathbf{H})\tilde{\mathbf{P}}_k \quad (24)$$

Where: $\mathbf{x}=[i_{s\alpha} \ i_{s\beta}]^T$: state vector; \mathbf{F} , \mathbf{H} : state transition matrix, measurement matrix; \mathbf{v} : zero-mean Gaussian measurement noise vector with covariance $\mathbf{R}=\sigma^2\mathbf{I}$; symbol \sim denotes predicted vectors.

4. RESULT AND DISCUSSION

Parameters of PMSM are listed in Table 2. Results are implemented in MATLAB/Simulink environment at $\omega_{m,ref}=150$ rpm, load torque jump= $0.5T_N$ (see Figure 3), values of covariance $\sigma^2=\{0.25^2, 0.5^2, 1.0^2, 2.0^2, 4.0^2\}$ (see Figures 4-5). Frequency converter has DC-link voltage of 372 Vdc, and switching frequency of 20 kHz. Performance of the proposed control structure and its conventional version without KF is evaluated by indices including ripples in forward operation (durations 0.2 s-0.3 s and 0.4 s-0.5 s) and reverse operation (durations 0.7 s-0.8 s and 0.9 s-1.0 s), the integral of the absolute value of speed error (IAE), the integral of time multiplied by the absolute value of speed error (ITAE) [26]-[28]:

$$IAE = \int_0^1 |e_\omega(t)| dt \quad (25)$$

$$ITAE = \int_0^1 t |e_\omega(t)| dt \quad (26)$$

Figures 4-5 show motor speeds in different cases of noise covariance σ^2 . It is easy to see that the larger parameter σ^2 , the higher ripple of motor speeds for both control structures. Table 3 indicates that the structure with KF brings reduction of 34%-81%, 53%-75% in motor speed ripple for forward and reverse operations respectively compared with the structure without KF, and the larger parameter σ^2 is, the more ripple tends to decrease. The ripples are only computed at the times when maximum value of absolute of speed error happens. Table 4 respectively show non-time-related and time-related performance indices IAE and ITAE. The structure with KF reduces 0.04%-64%, 0.06%-63% IAE, ITAE values than the structure without KF. Above evaluations show that the proposed structure owns much lower performance indices than the structure without KF. Reason for this is that filtered stator currents leads not only to smoother stator current responses, but also smaller ripples of stator fluxes and motor torque (see Figures 6-8). With large values 2.0², 4.0² of σ^2 , ripples of stator currents, stator fluxes and motor torque tend to increase, and it requires other approaches to lower the ripples, IAE, and ITAE.

Table 2. PMSM parameters [4]

Symbol	Quantity	Value
n_N	nominal speed	3000 rpm at $f=200$ Hz
T_N	nominal torque	7.73 Nm
P_N	nominal power	2.29 kW
J_m	motor inertia	0.00151 kgm ²
U_{lrms}	induced line-to-line voltage	263 V at 3000 rpm
I_{SN}	nominal stator current	5.6 A
ψ_M	magnetic flux of the PM	0.1706 Wb
P	number of pole pairs	4
R_s	stator resistance	0.65 Ω
L_s	stator inductance	7.7 mH

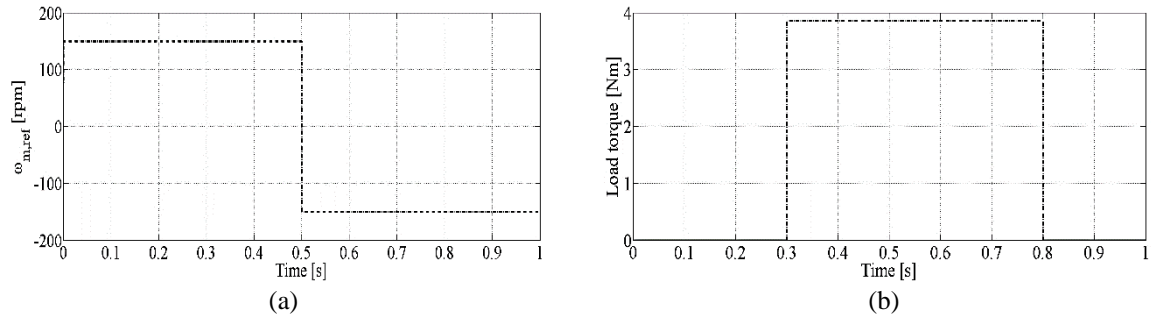


Figure 3. Reference (a) motor speed and (b) load torque

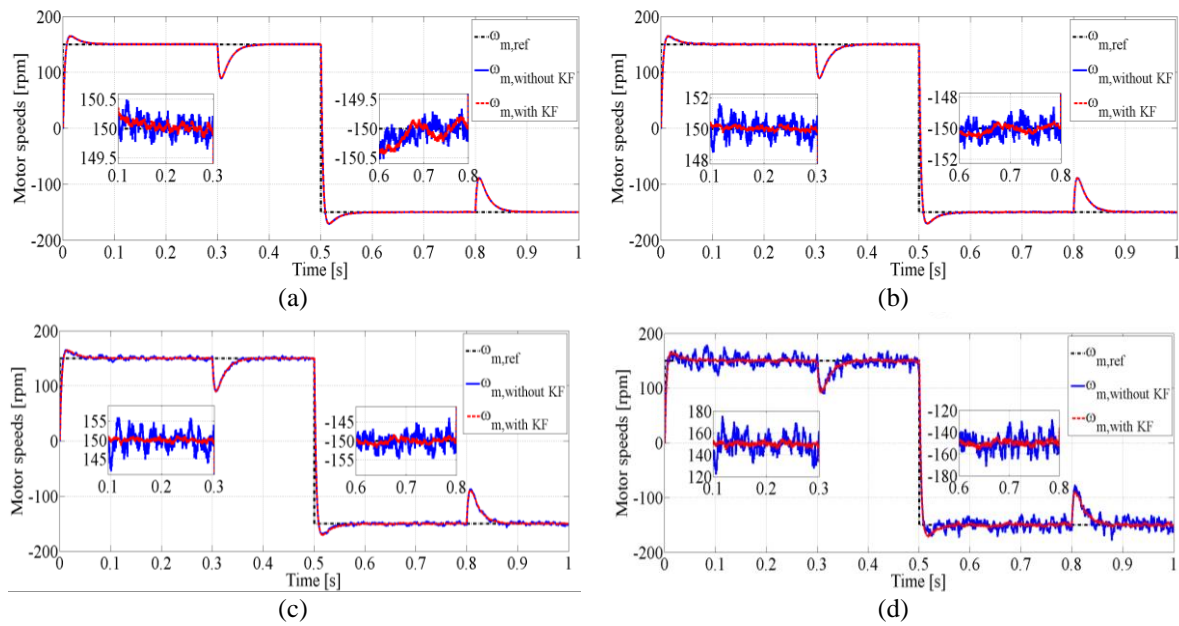


Figure 4. Motor speeds at (a) $\sigma^2=0.25^2$, (b) $\sigma^2=0.5^2$, (c) $\sigma^2=1.0^2$, and (d) $\sigma^2=2.0^2$

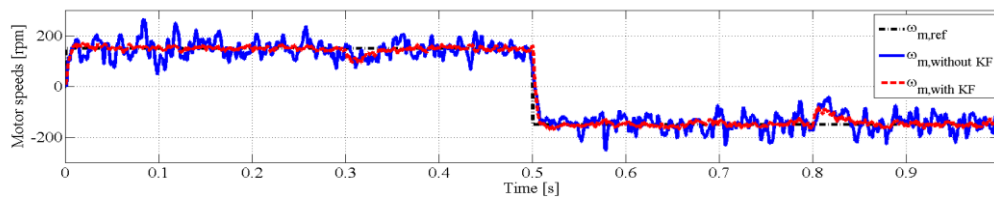


Figure 5. Motor speeds at $\sigma^2=4.0^2$

Table 3. Motor speed ripple [rpm]

σ^2	Forward operation		Reverse operation	
	Without KF	With KF	Without KF	With KF
0.25 ²	0.43	0.28	0.52	0.24
0.5 ²	1.50	0.39	1.48	0.47
1.0 ²	6.03	1.26	6.01	1.45
2.0 ²	22.75	5.03	21.46	6.13
4.0 ²	90.35	16.97	94.55	27.61

Table 4. IAE and ITAE performance indices

σ^2	Forward operation		Reverse operation	
	Without KF	With KF	Without KF	With KF
0.25 ²	5.425	5.423	2.568	2.567
0.5 ²	5.585	5.449	2.655	2.582
1.0 ²	6.343	5.595	3.057	2.662
2.0 ²	10.055	6.308	4.926	3.070
4.0 ²	27.792	9.739	13.579	4.953

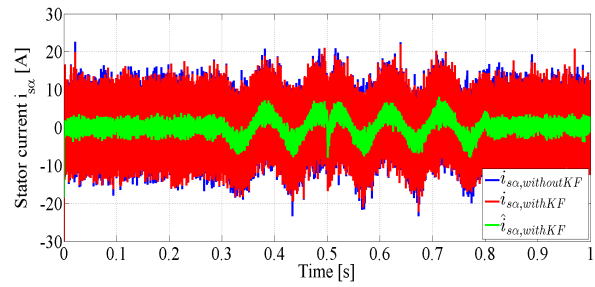
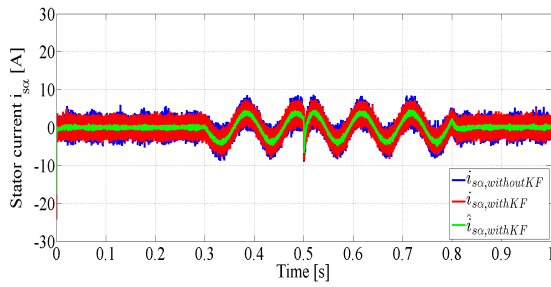


Figure 6. Stator currents $i_{s\alpha}$ at (a) $\sigma^2=1.0^2$ and (b) $\sigma^2=2.0^2$

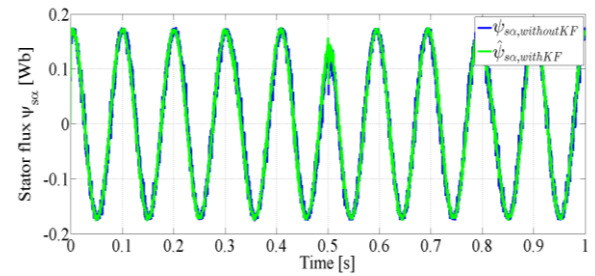
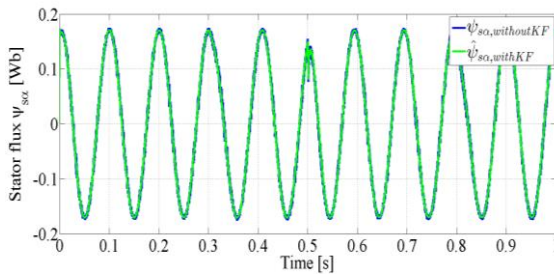


Figure 7. Stator fluxes $\psi_{s\alpha}$ at (a) $\sigma^2=1.0^2$ and (b) $\sigma^2=2.0^2$

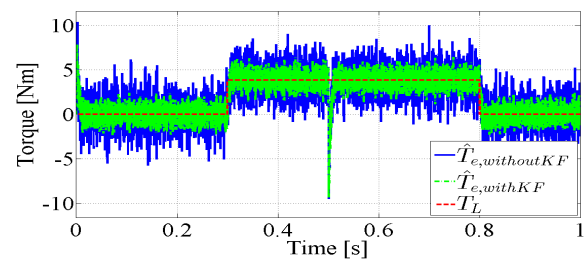
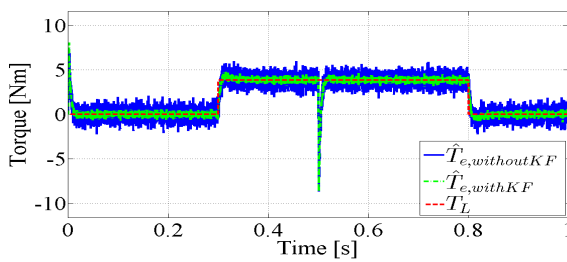


Figure 8. Torques at (a) $\sigma^2=1.0^2$ and (b) $\sigma^2=2.0^2$

5. CONCLUSION

The drive structure utilizing Kalman filtration and SVPWM of DTC PMSM drive was presented in the paper. Simulation results were carried out at a low reference speed, half of nominal torque, and large values of measurement noise covariance. The proposed structure dedicated significantly smaller performance indices including ripples, IAE and ITAE than the conventional drive structure without KF, especially at large covariances. It also provides smoother responses of stator current, stator flux, and motor torque compared to the structure without KF. Adaptive KFs can be employed to receive high-performance filtering. The proposed structure can be utilized in sensor or sensorless speed-control systems of PMSM drive using intelligent control, adaptive control or robust control.

REFERENCES




- [1] R. Hari Krishnan and A. E. George, "Direct Torque Control of PMSM using hysteresis modulation, PWM and DTC PWM based on PI Control for EV-A comparative analysis between the three strategies," *2019 2nd International Conference on Intelligent Computing, Instrumentation and Control Technologies (ICICICT)*, Kannur, India, 2019, pp. 566-571, doi: 10.1109/ICICICT46008.2019.8993271
- [2] F. Blaschke, "The Principle of Field Orientation as Applied to the New Transvektor Closed-Loop Control System for Rotating-Field Machines," *Siemens Review*, vol. 34, no. 3, 217-220, 1972.
- [3] M. Depenbrock, "Direct self-control (DSC) of inverter-fed induction machine," in *IEEE Transactions on Power Electronics*, vol. 3, no. 4, pp. 420-429, Oct. 1988, doi: 10.1109/63.17963.
- [4] P. Brandstetter, I. Neborak, M. Kuchar, "Analysis of Steady-State Error in Torque Current Component Control of PMSM Drive," *Advances in Electrical and Computer Engineering*, vol. 17, no. 2, pp. 39-46, 2017, doi: 10.4316/AECE.2017.02006.
- [5] C. Ming, G. Hanying and S. Hongming, "Simulation study on a DTC system of PMSM," *Proceedings of 2011 6th International Forum on Strategic Technology*, Harbin, Heilongjiang, 2011, pp. 564-569, doi: 10.1109/IFOST.2011.6021087.
- [6] Y. Yang, R. Hunag, Yan-pu Yu and S. Wang, "Direct torque control of permanent magnet synchronous motor based on space vector modulation control," *2016 IEEE 8th International Power Electronics and Motion Control Conference (IPEMC-ECCE Asia)*, Hefei, 2016, pp. 1818-1821, doi: 10.1109/IPEMC.2016.7512570.
- [7] H. H. Vo, "Application of MRAS Observer in Induction Motor Drive with Direct Torque Control" Ph.D. dissertation, VSB-Technical University of Ostrava, Ostrava, Czech Republic, 2017.
- [8] R. M. Patil, V. P. Dhote and A. Thosar, "Comparative Study of PWM Techniques to Feed Permanent Magnet Synchronous Motor," *2018 International Conference on Current Trends towards Converging Technologies (ICCTCT)*, Coimbatore, India, 2018, pp. 1-6, doi: 10.1109/ICCTCT.2018.8550906.
- [9] M. Khalid, A. Mohan and B. A. C. "Performance Analysis of Vector controlled PMSM Drive modulated with Sinusoidal PWM and Space Vector PWM," *2020 IEEE International Power and Renewable Energy Conference*, Karunagappally, India, 2020, pp. 1-6, doi: 10.1109/IPRECON49514.2020.9315210.
- [10] Q. Dong, B. Wang, Y. Yu, M. Tian, Z. Yun and D. Xu, "Hybrid PWM and Smooth Switching Technology for Traction PMSM Drives in Low Switching Frequency," *2020 IEEE 9th International Power Electronics and Motion Control Conference (IPEMC2020-ECCE Asia)*, Nanjing, China, 2020, pp. 2307-2312, doi: 10.1109/IPEMC-ECCEAsia48364.2020.9368160.
- [11] J. Xu and H. Zhang, "Random Asymmetric Carrier PWM Method for PMSM Vibration Reduction," in *IEEE Access*, vol. 8, pp. 109411-109420, 2020, doi: 10.1109/ACCESS.2020.3001288.
- [12] A. John and R. S. Kammala, "Optimal Selection of Switching Topology for PMSM Drive Based on Speed and Torque," *2021 13th IEEE PES Asia Pacific Power & Energy Engineering Conference (APPEEC)*, Thiruvananthapuram, India, 2021, pp. 1-6, doi: 10.1109/APPEEC50844.2021.9687769.
- [13] Z. Xiaorui, Z. Dongge and Z. Yiqi, "The Comparison of Two SVPWM Methods for Low-Speed Control of PMSM in Servo System," *2021 International Conference on Information Technology and Biomedical Engineering (ICITBE)*, Nanchang, China, 2021, pp. 207-211, doi: 10.1109/ICITBE54178.2021.00053.
- [14] H. H. Vo, P. Brandstetter, T. C. Tran, and C. S. T. Dong, "An Implementation of Rotor Speed Observer for Sensorless Induction Motor Drive in Case of Machine Parameter Uncertainty," *Advances in Electrical and Electronic Engineering*, vol. 16, no. 4, pp. 426-434, 2018, doi: 10.15598/aeec.v16i4.2973.
- [15] G. Liang *et al.*, "An Optimized Pulsewidth Modulation for Dual Three-Phase PMSM Under Low Carrier Ratio," in *IEEE Transactions on Power Electronics*, vol. 37, no. 3, pp. 3062-3072, March 2022, doi: 10.1109/TPEL.2021.3114304.
- [16] B. Wex, S. Silber, K. Kaspar and W. Gruber, "Fully Automated PWM Loss Calculation in Multiphase PMSM and Experimental Verification," in *IEEE Transactions on Industry Applications*, vol. 58, no. 4, pp. 4237-4247, July-Aug. 2022, doi: 10.1109/TIA.2022.3168048.
- [17] I. Djelamda and Ilhem Bouchareb, "Field-oriented control based on adaptive neuro-fuzzy inference system for PMSM dedicated to electric vehicle," *Bulletin of Electrical Engineering and Informatics*, vol. 11, no. 4, pp. 1892-1901, 2022, doi: 10.11591/eei.v11i4.3818.
- [18] S. Ye and X. Yao, "An Enhanced SMO-Based Permanent-Magnet Synchronous Machine Sensorless Drive Scheme With Current Measurement Error Compensation," in *IEEE Journal of Emerging and Selected Topics in Power Electronics*, vol. 9, no. 4, pp. 4407-4419, Aug. 2021, doi: 10.1109/JESTPE.2020.3038859.
- [19] H. H. Vo, D. Q. Nguyen, Q. T. Nguyen, C. S. T. Dong, T. C. Tran, P. Brandstetter, "Pulse-width modulation direct torque control induction motor drive with Kalman filter," *TELKOMNIKA Telecommunication, Computing, Electronics and Control*, vol. 19, no. 1, pp. 277-284, 2021, doi: 10.12928/telkomnika.v19i1.16247.
- [20] H. Chen, B. Liu, Y. Qu, X. Zhou, "Low speed control for PMSM based on reduced-order adaptive Kalman filter," in *33rd Chinese Control Conference*, Nanjing, 2014, pp. 7959-7963, doi: 10.1109/ChiCC.2014.6896330.
- [21] P. Brandstetter, M. Dobrovsky, M. Kuchar, C. S. T. Dong, H. H. Vo, "Application of BEMF-MRAS with Kalman Filter in Sensorless Control of Induction Motor Drive," *Electrical Engineering*, vol. 99, pp. 1151-1160, 2017, doi: 10.1007/s00202-017-0613-4.
- [22] Y. Li, M. Yang, J. Long, Z. Liu and D. Xu, "Current sensorless predictive control based on extended kalman filter for pmsm drives," *2017 IEEE Transportation Electrification Conference and Expo, Asia-Pacific (ITEC Asia-Pacific)*, Harbin, China, 2017, pp. 1-6, doi: 10.1109/ITEC-AP.2017.8080902.
- [23] Z. Liu, G. Feng and Y. Han, "Extended-Kalman-Filter-Based Magnet Flux Linkage and Inductance Estimation for PMSM Considering Magnetic Saturation," *2021 36th Youth Academic Annual Conference of Chinese Association of Automation (YAC)*, Nanchang, China, 2021, pp. 430-435, doi: 10.1109/YAC53711.2021.9486499.
- [24] X. Li and R. Kennel, "General Formulation of Kalman-Filter-Based Online Parameter Identification Methods for VSI-Fed PMSM," in *IEEE Transactions on Industrial Electronics*, vol. 68, no. 4, pp. 2856-2864, April 2021, doi: 10.1109/TIE.2020.2977568.
- [25] A. Kirad, S. Grouni and Y. Soufi, "Improved sensorless backstepping controller using extended Kalman filter of a permanent magnet synchronous machine," *Bulletin of Electrical Engineering and Informatics*, vol. 11, no. 2, pp. 658-671, 2022, doi: 10.11591/eei.v11i2.3560.
- [26] S. Manna and R. Mazumdar, "Comparative Performance Analysis of LQR and MPC for Active Suspension System," *2020 IEEE 5th International Conference on Computing Communication and Automation (ICCCA)*, Greater Noida, India, 2020, pp. 352-356, doi: 10.1109/ICCCA49541.2020.9250813.
- [27] P. Juneja *et al.*, "Design and Performance Analysis of Controllers based on Integral Error Criteria for a FOPDT Process Model," *2021 International Conference on Computational Performance Evaluation (ComPE)*, Shillong, India, 2021, pp. 086-089, doi:

10.1109/ComPE53109.2021.9752252.




- [28] S. Sengupta and C. Dey, "Auto-tuned Optimal PI Controllers for MIMO Processes," *2021 IEEE 4th International Conference on Computing, Power and Communication Technologies (GUCON)*, Kuala Lumpur, Malaysia, 2021, pp. 1-6, doi: 10.1109/GUCON50781.2021.9752252.

BIOGRAPHIES OF AUTHORS






Dung Quang Nguyen    received his MSc degree from Tomsk Polytechnic University, Tomsk City, Russia in 2012. He is now a PhD Student at Faculty of Electrical and Electronics Engineering (FEEE), Ton Duc Thang University (TDTU), Vietnam. His research interests include applications of Kalman filter in control systems; identification and synthesis in fractional, distributed parameter systems; non-linear system. He can be contacted at email: nguyenquangdung@tdtu.edu.vn.



Hau Huu Vo    hold a PhD degree from Faculty of Electrical Engineering and Computer Science (FEECS), Technical University of Ostrava (VSB-TUO), Czech Republic in 2017. He is currently a Lecturer at FEEE, TDTU. He has published 10 journal papers. His research interests are modern electrical drives. He can be contacted at email: vohuuha@tdtu.edu.vn.



Pavel Brandstetter    received his PhD degree at Brno University in 1987. He is now full professor at FEECS, VSB-TUO, Czech Republic. He has published more than 65 conference papers and 30 journal papers. His research interests are intelligent methods in electrical drives and power electronics. He can be contacted at email: pavel.brandstetter@vsb.cz.